Filling and Beam Loading in TESLA Superstructures

M. Dohlus
(DESY)

H.W. Glock, D. Hecht, U. van Rienen
(Institut für Allgemeine Elektrotechnik, Universität Rostock)

Abstract: The so-called superstructure is a chain of 4 coupled 7-cell cavities driven by a single input coupler. Therefore the question of proper filling and refilling with field energy is of great importance. In this report, we present calculations based on an eigenmode expansion to determine the transient field behaviour. A comparison with the traditional 9-cell structure is given.

1. Overview

In order to calculate the time dependent behaviour of the fields inside the superstructure we use an expansion into a set of eigenmodes. The eigenmodes, their frequencies, field energies and beam relevance are calculated numerically, in our case with MAFIA [1]. Details of these calculations are given in section 3. Using their results one can set up a system of coupled ordinary differential equations with a solution explictly given. For the reason of completeness details of this method, which is not restricted to a certain resonator geometry and which has been used already from various authors ([2], [3], [4]), are given in section 2. Section 4 contains the results on the 4x7-superstructure and its underlying assumptions and a comparison with the well-established 9-cell-structure.

The same problem concerning the 4x7-superstructure (and furthermore a 4x9-structure to compare with measurements) was calculated already from Ferrario and Sekutowicz ([5], [6]). Their method was quite similar; differences are caused mainly by the use of a different code to calculate the resonator modes and some details of theoretical modelling. There is no difference in the general conclusions.

2. Model and Theory

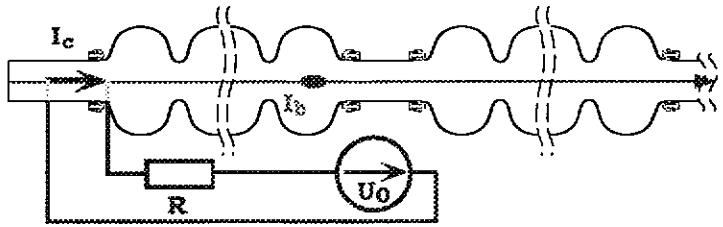

Fig. 1: Schematic overview of the model (compare main text). The cavity geometry is mirrored at the right border in order to calculate a four-cavity-chain. The transmitter-driven current I_c has a fixed (arbitrarily chosen) location near the left end of the first cavity whereas the beam current I_b traverses all four cavities.

Figure 1 summarizes the effects that are taken into account in the model: Together with the resistor R an ideal rf voltage source switched on at t = 0 with constant amplitude U_0 is coupled to the cavity. This coupling is simulated as an on-axis current path located in the beam pipe near the first cell. In this manner the input coupler is substituted, assuming a common factor for all modes between peripheral fields acting on the real input coupler and the on-axis-fields. This simplifies the field data extraction from the numerical calculation. Length and location of the current path are chosen arbitrarily. The Q-value of the accelerating mode, which has to be the design value (comp. section 4), is adjusted with the transmitter resistance R.

The beam is simulated as a sequence of Dirac pulses with velocity of light, traversing along the cavity axis. To evaluate the field excitation the on-axis profiles of all modes are needed. Due to the large frequency gap to higher monopole modes the mode system is restricted to the fundamental passband.

Taking into account the assumptions noted above the relevant equations will now be derived. Starting from Maxwells equations

$$\nabla \times \vec{H} = \vec{j} + \partial_t \vec{D} \qquad \nabla \times \vec{E} = -\partial_t \vec{B} \qquad (1\ a, b)$$

$$\Downarrow$$

$$\nabla \times \frac{1}{\mu} \nabla \times \vec{E} = -\partial_t (\nabla \times \vec{H})$$

$$\Downarrow \qquad\qquad \Downarrow$$

$$\nabla \times \frac{1}{\mu} \nabla \times \vec{E} + \varepsilon \partial_t^2 \vec{E} = -\partial_t \vec{j}$$

working in cartesian coordinates and for vanishing sources of $\vec{E}$ the first expression on the left hand side results in

$$\nabla \times \frac{1}{\mu} \nabla \times \vec{E} = \frac{1}{\mu} \left(\nabla(\nabla \cdot \vec{E}) - \Delta \vec{E}\right) = -\frac{1}{\mu} \Delta \vec{E}$$

which finally yields:

$$-\frac{1}{\mu} \Delta \vec{E} + \varepsilon \partial_t^2 \vec{E} = -\partial_t \vec{j} \qquad (2)$$

The total electrical field is expanded in a set of eigenmodes $\vec{E}_\nu(\vec{r})$

$$\vec{E}(\vec{r},t) = \sum_\nu a_\nu(t) \frac{\vec{E}_\nu(\vec{r})}{\sqrt{2\,W_\nu}} \qquad (3)$$

with time dependent amplitudes $a_\nu(t)$ and field energies W_ν. Each of the eigenmodes is a solution of

$$\Delta \vec{E}_\nu + k_\nu^2 \vec{E}_\nu = 0 \quad \text{with} \quad k_\nu^2 = \omega_\nu^2\, \varepsilon\mu$$

which is the wave equation and therefore:

$$-\frac{1}{\mu} \Delta \vec{E} + \varepsilon \partial_t^2 \vec{E} = \varepsilon \sum_\nu \left[\frac{\vec{E}_\nu(\vec{r})}{\sqrt{2\,W_\nu}} \left(\omega_\nu^2 + \partial_t^2\right) a_\nu(t) \right] = -\partial_t \vec{j} \qquad (4)$$

Applying the orthogonality relation of the eigenmodes

$$\iiint_{V_{res}} \varepsilon\, \vec{E}_\xi \vec{E}_\zeta \, dV = 2\delta_{\xi\zeta}\, W_\zeta$$

to the right equation in (4) yields (replace $\zeta \rightarrow \nu$):

$$\left(\omega_\nu^2 + \partial_t^2\right) a_\nu(t) = -\partial_t \iiint_{V_{res}} \frac{\vec{j}(\vec{r},t)\, \vec{E}_\nu(\vec{r})}{\sqrt{2\,W_\nu}} \, dV =: -\partial_t\, c_\nu(t) \qquad (5)$$

The density of the externally driven currents $\vec{j}(\vec{r},t)$ has two distinct contributions from the beam ($\vec{j}_b(\vec{r},t)$) and the transmitter coupled current ($\vec{j}_c(\vec{r},t)$):

$$\vec{j}(\vec{r},t) = \vec{j}_b(\vec{r},t) + \vec{j}_c(\vec{r},t) \qquad (6)$$

According to Definition (5) the coefficient of the driving current $c_\nu(t)$ can be splitted up in the same manner:

$$c_\nu(t) = c_{\nu,b}(t) + c_{\nu,c}(t) \qquad (7)$$

In case of an on-axis beam with constant velocity v it follows:

$$c_{\nu,b}(t) = \iiint_{V_{res}} \frac{\vec{j}_b(\vec{r},t)\, \vec{E}_\nu(\vec{r})}{\sqrt{2\,W_\nu}} \, dV = \iiint_{V_{res}} \frac{\left[\delta(x)\,\delta(y)\, I_b(t - \frac{z}{v})\, \vec{e}_z\right] \vec{E}_\nu(\vec{r})}{\sqrt{2\,W_\nu}} \, dV =$$

$$= \int_{z\text{-axis}} \frac{I_b(t - \frac{z}{v})\, \vec{e}_z\, \vec{E}_\nu(\vec{r})}{\sqrt{2\,W_\nu}} \, dz \qquad (8)$$

The current driven from the transmitter is assumed to be one-dimensional and constant along its path. Therefore

$$c_{\nu,c}(t) = \iiint_{V_{res}} \frac{\vec{j}_c(\vec{r},t)\, \vec{E}_\nu(\vec{r})}{\sqrt{2\,W_\nu}} \, dV = I_c(t) \frac{\int_{\text{curr.-path}} \vec{E}_\nu(\vec{r})\, d\vec{r}}{\sqrt{2\,W_\nu}} \qquad (9)$$

holds. Applying Kirchhoffs law on the external transmitter circuit (comp. Fig. 1) one finds:

$$U_c(t) + R\, I_c(t) = U_0(t) \qquad (10)$$

With the abbrevation

$$K_\nu := \frac{\int_{\text{curr.-path}} \vec{E}_\nu(\vec{r})\, d\vec{r}}{\sqrt{2\,W_\nu}} \qquad (11)$$

the correlation between the voltage $U_c(t)$ at the resonator port and the mode amplitudes may be written as

$$U_c(t) = -\sum_\nu a_\nu(t) \frac{\int_{\text{curr.-path}} \vec{E}_\nu(\vec{r})\, d\vec{r}}{\sqrt{2\,W_\nu}} = -\sum_\nu a_\nu(t)\, K_\nu \qquad (12)$$

and the coefficients of the driving current given in (9) can be expressed as:

$$c_{\nu,c}(t) = I_c(t) \frac{\int_{\text{curr.-path}} \vec{E}_\nu(\vec{r})\, d\vec{r}}{\sqrt{2\,W_\nu}} = I_c(t)\, K_\nu \qquad (13)$$

Equ. (10) reads together with (12)

$$-\frac{1}{R} \sum_\nu a_\nu(t)\, K_\nu + I_c(t) = \frac{U_0(t)}{R}$$

and its time derivative as

$$-\frac{1}{R} \sum_\nu \partial_t\, a_\nu(t)\, K_\nu + \partial_t\, I_c(t) = \frac{\partial_t\, U_0(t)}{R}$$

or:

$$\partial_t\, I_c(t) = \frac{\partial_t\, U_0(t)}{R} + \frac{1}{R} \sum_\nu \partial_t\, a_\nu(t)\, K_\nu \qquad (14)$$

Equ. (5) with (13), (14) lead further to:

$$\left(\omega_\nu^2 + \partial_t^2\right) a_\nu(t) = -\partial_t\, c_\nu(t) =$$

$$= -\partial_t\, c_{\nu,b}(t) - \partial_t\, c_{\nu,c}(t) =$$

$$= -\partial_t\, c_{\nu,b}(t) - \partial_t\, I_c(t)\, K_\nu =$$

$$= -\partial_t\, c_{\nu,b}(t) - K_\nu \left[\frac{\partial_t\, U_0(t)}{R} + \frac{1}{R} \sum_m \partial_t\, a_\nu(t)\, K_m\right]$$

After rearranging the left hand side this reads as:

$$\left(\omega_\nu^2 + \partial_t^2\right) a_\nu(t) + \frac{1}{R} \sum_m K_\nu K_m \partial_t a_\nu(t) = -\partial_t \left[c_{\nu,b}(t) + \frac{K_\nu}{R} U_0(t) \right] \quad \forall\, \nu \qquad (15)$$

Equ. (15) establishes a system of second order differential equations in the mode amplitudes $a_\nu(t)$. Obviously its homogeneous part describes a set of coupled oscillators. The right hand side contains the excitation of the system induced by beam and transmitter. Introducing a second set of variables the solution is technically simplified:

$$b_\nu := \frac{1}{i\,\omega_\nu} \partial_t a_\nu \quad \Leftrightarrow \quad \partial_t a_\nu = i\,\omega_\nu b_\nu \quad \Leftrightarrow \quad \partial_t^2 a_\nu = i\,\omega_\nu \partial_t b_\nu \qquad (16\,a\text{-}c)$$

Replacing $\partial_t^2 a_\nu$ and $\partial_t a_\nu$ in (15) according to (16 b,c) and dividing by $i\,\omega_\nu$ yields using (16) a set of two equations belonging to the same index:

$$\begin{aligned} &\partial_t a_\nu - i\,\omega\, a_\nu = 0 \\ &\partial_t b_\nu + \sum_m \frac{K_\nu K_m \omega_m}{R\,\omega_\nu} b_m - i\,\omega\, a_\nu = \frac{i}{\omega_\nu} \partial_t \left[c_{\nu,b}(t) + \frac{K_\nu}{R} U_0(t) \right] \end{aligned} \qquad (17\,a,b)$$

The inhomogenity in (17 b) is abbreviated as:

$$s_\nu := \frac{i}{\omega_\nu} \partial_t \left[c_{\nu,b}(t) + \frac{K_\nu}{R} U_0(t) \right] \qquad (18)$$

Written as matrix-vector relation the system (17) reads like:

$$\partial_t \begin{pmatrix} a_1 \\ b_1 \\ \vdots \\ a_n \\ b_n \end{pmatrix} - \begin{pmatrix} 0 & i\,\omega_1 & \cdots & 0 & 0 \\ i\,\omega_1 & -\frac{K_1^2}{R} & \cdots & 0 & -\frac{K_1 K_n \omega_n}{R\,\omega_1} \\ \vdots & \vdots & & \vdots & \vdots \\ 0 & 0 & \cdots & 0 & i\,\omega_n \\ 0 & -\frac{K_n K_1 \omega_1}{R\,\omega_n} & \cdots & i\,\omega_n & -\frac{K_n^2}{R} \end{pmatrix} \begin{pmatrix} a_1 \\ b_1 \\ \vdots \\ a_n \\ b_n \end{pmatrix} = \begin{pmatrix} 0 \\ s_1 \\ \vdots \\ 0 \\ s_n \end{pmatrix} \qquad (19)$$

As commonly known the solution of a homogeneous system

$$\partial_t \vec{v} - \underline{\underline{M}}\, \vec{v} = 0 \qquad (20)$$

is given as:

$$\vec{v}(t) = \sum_{j=1}^{2n} \left(\vec{e}_j\, e^{\lambda_j t}\, u_j \right) \qquad (21)$$

Herein λ_j are the eigenvalues and $\vec{e}_j$ the corresponding eigenvectors of the matrix $\underline{\underline{M}}$. These eigenvalues and eigenvectors have to be calculated numerically (which is - besides the field simulations (sect. 3) - the only non-analytical step in the calculation). The quantities u_j are arbitrary but constant amplitudes. To solve the inhomogeneous system

$$\partial_t \vec{v} - \underline{\underline{M}}\, \vec{v} = \vec{s} \qquad (22)$$

with the right hand side:

$$\vec{s} = \begin{pmatrix} 0 \\ s_1 \\ \vdots \\ 0 \\ s_n \end{pmatrix}$$

these amplitudes are assumed to be time-dependent:

$$\vec{v}(t) = \sum_{j=1}^{2n} \left(\vec{e}_j\, e^{\lambda_j t}\, u_j(t) \right) \qquad (23)$$

Equ. (23) may be written in matrix-vector-notation

$$\vec{v}(t) = \left(\vec{e}_1, \cdots, \vec{e}_{2n} \right) \begin{pmatrix} e^{\lambda_1 t} & & \\ & \ddots & \\ & & e^{\lambda_{2n} t} \end{pmatrix} \begin{pmatrix} u_1(t) \\ \vdots \\ u_{2n}(t) \end{pmatrix} = \underline{\underline{V}} \begin{pmatrix} e^{\lambda_1 t} & & \\ & \ddots & \\ & & e^{\lambda_{2n} t} \end{pmatrix} \begin{pmatrix} u_1(t) \\ \vdots \\ u_{2n}(t) \end{pmatrix} \qquad (24)$$

introducing the column matrix of the eigenvectors:

$$\underline{\underline{V}} = \left(\vec{e}_1, \cdots, \vec{e}_{2n} \right) \qquad (25)$$

Then the time derivative in (22) reads like

$$\partial_t \vec{v} = \underline{\underline{V}} \begin{pmatrix} e^{\lambda_1 t} & & \\ & \ddots & \\ & & e^{\lambda_{2n} t} \end{pmatrix} \left[\begin{pmatrix} \lambda_1 & & \\ & \ddots & \\ & & \lambda_{2n} \end{pmatrix} \begin{pmatrix} u_1(t) \\ \vdots \\ u_{2n}(t) \end{pmatrix} + \partial_t \begin{pmatrix} u_1(t) \\ \vdots \\ u_{2n}(t) \end{pmatrix} \right]$$

and the second term as:

$$\begin{aligned} \underline{\underline{M}}\, \vec{v} &= \underline{\underline{M}} \left(\vec{e}_1, \cdots, \vec{e}_{2n} \right) \begin{pmatrix} e^{\lambda_1 t} & & \\ & \ddots & \\ & & e^{\lambda_{2n} t} \end{pmatrix} \begin{pmatrix} u_1(t) \\ \vdots \\ u_{2n}(t) \end{pmatrix} = \\ &= \left(\lambda_1 \vec{e}_1, \cdots, \lambda_{2n} \vec{e}_{2n} \right) \begin{pmatrix} e^{\lambda_1 t} & & \\ & \ddots & \\ & & e^{\lambda_{2n} t} \end{pmatrix} \begin{pmatrix} u_1(t) \\ \vdots \\ u_{2n}(t) \end{pmatrix} = \\ &= \left(\vec{e}_1, \cdots, \vec{e}_{2n} \right) \begin{pmatrix} e^{\lambda_1 t} & & \\ & \ddots & \\ & & e^{\lambda_{2n} t} \end{pmatrix} \begin{pmatrix} \lambda_1 & & \\ & \ddots & \\ & & \lambda_{2n} \end{pmatrix} \begin{pmatrix} u_1(t) \\ \vdots \\ u_{2n}(t) \end{pmatrix} \end{aligned}$$

Altogether this yields

$$\underline{\underline{V}} \begin{pmatrix} e^{\lambda_1 t} & & \\ & \ddots & \\ & & e^{\lambda_{2n} t} \end{pmatrix} \partial_t \begin{pmatrix} u_1(t) \\ \vdots \\ u_{2n}(t) \end{pmatrix} = \begin{pmatrix} 0 \\ s_1 \\ \vdots \\ 0 \\ s_n \end{pmatrix} \qquad (26)$$

which may be integrated either completely:

$$\begin{pmatrix} u_1(t) \\ \vdots \\ u_{2n}(t) \end{pmatrix} = \int_{\tau=-\infty}^{t} \begin{pmatrix} e^{-\lambda_1 \tau} & & \\ & \ddots & \\ & & e^{-\lambda_{2n} \tau} \end{pmatrix} \underline{\underline{V}}^{-1} \begin{pmatrix} 0 \\ s_1(\tau) \\ \vdots \\ 0 \\ s_n(\tau) \end{pmatrix} d\tau \qquad (27)$$

or - with the advantage of shorter expressions - by means of Cramers rule:

$$u_j(t) = \frac{\det\left(\vec{e}_1, \ldots, \int_{\tau=-\infty}^{t} e^{-\lambda_j \tau}\, \vec{s}(\tau)\, d\tau, \ldots, \vec{e}_{2n}\right)}{\det\left(\vec{e}_1, \ldots, \vec{e}_{2n}\right)} \tag{28}$$

The vector which holds the time dependent quantities will be refered as:

$$\vec{W}_j(t) = \int_{\tau=-\infty}^{t} e^{-\lambda_j \tau}\, \vec{s}(\tau)\, d\tau \tag{29}$$

All excitations of the system start with $t = 0$, so using (18) this yields:

$$\vec{W}_j(t) = \int_{\tau=0}^{t} e^{-\lambda_j \tau} \begin{pmatrix} \vdots \\ 0 \\ \frac{i}{\omega_v}\partial_\tau\left[c_{v,b}(\tau) + \frac{K_v}{R} U_0(\tau)\right] \\ \vdots \end{pmatrix} d\tau$$

Again the two different contributions of beam (index b) and transmitter current (index c) are separated:

$$\begin{aligned} \vec{W}_j(t) &= \int_{\tau=0}^{t} e^{-\lambda_j \tau} \begin{pmatrix} \vdots \\ 0 \\ \frac{i}{\omega_v}\partial_\tau c_{v,b}(\tau) \\ \vdots \end{pmatrix} d\tau + \frac{i}{R}\int_{\tau=0}^{t} e^{-\lambda_j \tau} \begin{pmatrix} \vdots \\ 0 \\ K_v/\omega_v \\ \vdots \end{pmatrix} \partial_\tau U_0(\tau)\, d\tau = \\ &= \vec{W}_{b,j}(t) + \vec{W}_{c,j}(t) \end{aligned} \tag{30}$$

The transmitter current is assumed to have the time dependency

$$U_0(t) = V_0\, e^{+i\omega_0 t} \tag{31}$$

which, using the abbreviation

$$\vec{K} = \begin{pmatrix} \vdots \\ 0 \\ K_v/\omega_v \\ \vdots \end{pmatrix}, \tag{32}$$

allows for an explicit integration of $\vec{W}_{c,j}(t)$:

$$\begin{aligned} \vec{W}_{c,j}(t) &= \frac{i}{R}\vec{K}\int_{\tau=0}^{t} e^{-\lambda_j \tau}\partial_\tau\left(V_0\, e^{+i\omega_0 \tau}\right) d\tau = \\ &= \frac{V_0}{R}\vec{K}\,\frac{\omega_0}{i\omega_0 - \lambda_j}\left[1 - e^{(i\omega_0 - \lambda_j)t}\right] \end{aligned} \tag{33}$$

In order to evaluate the beam excitation

$$\vec{W}_{b,j}(t) = \int_{\tau=0}^{t} e^{-\lambda_j \tau} \begin{pmatrix} \vdots \\ 0 \\ \frac{i}{\omega_v}\partial_\tau c_{v,b}(\tau) \\ \vdots \end{pmatrix} d\tau$$

one has to use Equ. (8)

$$c_{v,b}(t) = \int_{z-\text{axis}} \frac{I_b(t - \frac{z}{v})\, \vec{e}_z \vec{E}_v(\vec{r})}{\sqrt{2\, W_v}}\, dz$$

with $I_b(t)$ being the (particle) current at time t and $z = 0$. No excitation has happened before $t = 0$, so $I_b(t < 0) = 0$. A δ-pulse of a single charge q, traversing $z = 0$ at $t = t_b$ is given by

$$I_{b,\delta}(t) = q\,\delta(t - t_b) \tag{34}$$

and consequently:

$$\begin{aligned} c_{v,b,\delta}(t) &= \int_{z-\text{axis}} \frac{q\,\delta(t - t_b - \frac{z}{v})\, \vec{e}_z \vec{E}_v(\vec{r})}{\sqrt{2\, W_v}}\, dz = \\ &= \frac{q\,v}{\sqrt{2\, W_v}} E_{z,v}(v\,(t - t_b)) \begin{Bmatrix} 1 \text{ if } 0 \le (t - t_b) \le \frac{L_{res}}{v} \\ 0 \text{ otherwise} \end{Bmatrix} =: \\ &=: \frac{q\,v}{\sqrt{2\, W_v}} E_{z,v}(v\,(t - t_b))\, \Psi\left[{}^{L_{res}}\!/_{v};\, (t - t_b)\right] \end{aligned} \tag{35}$$

$\Psi\left[{}^{L_{res}}\!/_{v};\, (t - t_b)\right]$ contains the double step function needed in (35). In case of such a single charge excitation the corresponding component of $\vec{W}_{b,j}(t)$ reads like:

$$\begin{aligned} W_{b,j,v} &= \int_{\tau=0}^{t} e^{-\lambda_j \tau}\frac{i}{\omega_v}\partial_\tau\left[\frac{q\,v}{\sqrt{2\, W_v}} E_{z,v}(v\,(\tau - t_b))\, \Psi\left[{}^{L_{res}}\!/_{v};\, (\tau - t_b)\right]\right] d\tau = \\ &= \frac{i\,q\,v}{\omega_v\sqrt{2\, W_v}}\int_{\tau=0}^{t} e^{-\lambda_j \tau}\,\partial_\tau\left[E_{z,v}(v\,(\tau - t_b))\, \Psi\left[{}^{L_{res}}\!/_{v};\, (\tau - t_b)\right]\right] d\tau = \\ &= \frac{i\,q\,v}{\omega_v\sqrt{2\, W_v}}\left\{\left[e^{-\lambda_j \tau} E_{z,v}(v\,(\tau - t_b))\, \Psi\left[{}^{L_{res}}\!/_{v};\, (t - t_b)\right]\right]\Big|_{\tau=0}^{t} - \right. \\ &\qquad \left. - (-\lambda_j)\int_{\tau=0}^{t} e^{-\lambda_j \tau} E_{z,v}(v\,(\tau - t_b))\, \Psi\left[{}^{L_{res}}\!/_{v};\, (\tau - t_b)\right] d\tau\right\} \end{aligned} \tag{36}$$

Herein the second step results from an integration by parts. The remaining integral is transformed using the substitution $\tau' = \tau - t_b$:

$$\int_{\tau=0}^{t} e^{-\lambda_j \tau} E_{z,\nu}(v(\tau - t_b))\, \Psi[{}^{L_{res}}\!/_{v};\, (\tau - t_b)]\, d\tau = \int_{\tau'=-t_b}^{t-t_b} e^{-\lambda_j (\tau' + t_b)} E_{z,\nu}(v\tau')\, \Psi[{}^{L_{res}}\!/_{v};\, \tau']\, d\tau' =$$

$$\tau' \to \tau \qquad = e^{-\lambda_j t_b} \int_{\tau=-t_b}^{t-t_b} e^{-\lambda_j \tau} E_{z,\nu}(v\tau)\, \Psi[{}^{L_{res}}\!/_{v};\, \tau]\, d\tau =$$

$$= e^{-\lambda_j t_b} \int_{\tau=0}^{t_{max}} e^{-\lambda_j \tau} E_{z,\nu}(v\tau)\, d\tau$$

$$\text{with } t_{max} = \begin{cases} (t - t_b) & \text{if } 0 < (t - t_b) < \frac{L_{res}}{v} \Leftrightarrow t_b < t < \frac{L_{res}}{v} + t_b \\ \frac{L_{res}}{v} & \text{if } t > \frac{L_{res}}{v} + t_b \end{cases} \qquad (37)$$

In the last step the time of entering the cavity t_b of each bunch is separated from the integration. From now on we partly restrict ourselves to these time intervals without a charge inside the cavity. Then $t_{max} = {}^{L_{res}}\!/_{v}$ holds and the integral in (37) becomes time independent. Futhermore the integrated term in (36) then vanishes. During a charge traversal the result is incomplete since the postition/time-dependent contribution of this single charge is not counted. It is added totally after the charge left the resonator and from then on the result again is correct. One of us (M.Dohlus) added the contribution for all points of time in a special code.

In the case of several bunches all their excitations (as long as they have left the resonator at time t) have to be summed up. So (36) has to be modified (including the simplification mentioned above)

$$W_{b,j,\nu} = \frac{i\, q\, v\, \lambda_j}{\omega_\nu \sqrt{2\, W_\nu}} \left(\int_{\tau=0}^{{}^{L_{res}}\!/_{v}} e^{-\lambda_j \tau} E_{z,\nu}(v\tau)\, d\tau \right) \left(\sum_{t_b < (t - {}^{L_{res}}\!/_{v})} e^{-\lambda_j t_b} \right) \qquad (38)$$

or written as vector:

$$\vec{W}_{b,j} = i\, q\, v\, \lambda_j \left(\sum_{t_b < (t - {}^{L_{res}}\!/_{v})} e^{-\lambda_j t_b} \right) \begin{pmatrix} \vdots \\ 0 \\ \frac{1}{\omega_\nu \sqrt{2\, W_\nu}} \left(\int_{\tau=0}^{{}^{L_{res}}\!/_{v}} e^{-\lambda_j \tau} E_{z,\nu}(v\tau)\, d\tau \right) \\ \vdots \end{pmatrix} \qquad (39)$$

Only the summation has to be evaluated with respect to the beam structure. All other quantities in (39) are calculated from cavity properties and remain unchanged.

The solution of the mode amplitudes originally searched for is found summarizing the above calculations:

$$\begin{pmatrix} a_1(t) \\ b_1(t) \\ \vdots \\ a_n(t) \\ b_n(t) \end{pmatrix} = \frac{1}{\det \underline{V}} \sum_{j=1}^{2n} \left[\vec{e}_j\, e^{\lambda_j t} \det \left(\vec{e}_1, \cdots, \left(\vec{W}_{b,j}(t) + \vec{W}_{c,j}(t) \right), \cdots, \vec{e}_{2n} \right) \right] \qquad (40)$$

In the general case of simultaneous beam and transmitter excitation further replacement of (33) and (39) within (40) does not simplify neither formal representation nor calculation. For vanishing beam a somewhat shorter expression may be found:

$$\begin{pmatrix} a_1(t) \\ b_1(t) \\ \vdots \\ a_n(t) \\ b_n(t) \end{pmatrix}_{\text{no beam}} = \frac{V_0\, \omega_0}{R \det \underline{V}} \sum_{j=1}^{2n} \left[\vec{e}_j \frac{e^{\lambda_j t} - e^{i\omega_0 t}}{\omega_0 + i\, \lambda_j} \det \left(\vec{e}_1, \ldots, \vec{K}, \ldots, \vec{e}_{2n} \right) \right] \qquad (41)$$

$\vec{K}$ (found from (32) and (11)) replaces $\vec{e}_j$ in the determinant

The total time dependent electric field is then derived from (3):

$$\vec{E}(\vec{r}, t) = \sum_\nu a_\nu(t) \frac{\vec{E}_\nu(\vec{r})}{\sqrt{2\, W_\nu}} \qquad (3)$$

With the last step the original problem is formally solved.

It is useful to analyze (41) with respect to the special case of excitation at one of the eigenfrequencies: All eigenvalues of the system matrix (compare (19)) have the form:

$$\lambda_j = -\alpha_j (\mp)\, \omega_j \qquad (42)$$

They appear in pairs with the same negative real part - describing the damping - and both signs of the imaginary parts. If we decide to use an excitation frequency ω_0 with positive sign all eigenmodes with positive ω_j will reach only very low amplitudes due to the denominator in (41). In the special case $\omega_0 = -\omega_j$ the eigenvector $\vec{e}_j$ is strongly dominating the sum. Then the field profile $\vec{E}_j$ dominates the total field since $\vec{e}_j$ has only small $a_{k,k \neq j}$.

With increasing time t all $e^{\lambda_j t}$-terms vanish. The corresponding Q-values can directly be found from the eigenvalues (42):

$$Q_j = \frac{\omega_j}{2\, \alpha_j} = \frac{|\mathrm{Im}(\lambda_j)|}{2\, \mathrm{Re}(\lambda_j)} \qquad (43)$$

3. MAFIA Eigenmode Calculation

As seen in the previous section the following set of quantities characterizing the eigenmodes is needed:

- the eigenfrequency $f_j = \frac{\omega_j}{2\pi}$
- the stored energy W_j
- the E_z-profile at the beam path (in our case on-axis)
- the E-field at the location and in direction of the externally driven current (in our case a short on-axis-path at the cavity front; identical to the E_z-profile in this range)

Due to the cavity geometry these quantities have to be determined numerically, in our case with MAFIA. Even exploiting the symmetry of the superstructure the problem size is reasonable high. In order to model the boundary curvature avoiding stair case approximations, yet with limited number of mesh points, a command file was written that calculates appropriate z-mesh lines for given r-mesh lines.

The basic idea is illustrated in the following excerpt of the command file written in the MAFIA programming language.

```
...

if (rlinad .ge. rw .and. rlinad .lt. ru) then
   define zlinad = "a*sqrt(1-((rlinad-rb)/b)**2)"
   zadd zlinad exec
endif
if (rlinad .ge. ru .and. rlinad .lt. ro) then
   define zlinad = "zu+(zo-zu)/(ro-ru)*(rlinad-ru)"
   zadd zlinad exec
endif
if (rlinad .ge. ro) then
   define zlinad = "zh - sqrt(c**2 - (rlinad-rk)**2)"
   zadd zlinad exec
endif

...
```

In a sequence of three "if"-clauses it is decided whether a given r-mesh line at radius `rlinad` crosses the cavity boundary in its elliptic, linear or circular part (comp. fig. 2). Then `zlinad`, the position of the z-meshline to add, is calculated using the geometric parameters of the respective shape. They are known for all different cell shapes (left end- and left intermediate-cell of end resonator; standard end-, standard intermediate–, standard inner-cell of inner resonator; right cells mirrored to left ones) - compare table 1.

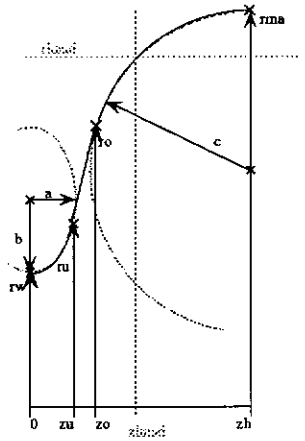

Fig. 2: Shape of a half cell, composed of elliptic, linear and circular part with a single radial meshline at r = rlinad and a z-meshline crossing the shape in the same point.

half cell type	ee	ei	se	si	in
rw	57.00	35.00	57.00	35.00	35.00
ru	64.3851	47.7900	64.3851	47.7765	47.3910
zu	11.4573	11.3410	11.4573	11.3880	11.2510
ro	81.6601	71.9564	81.6524	71.9183	70.9020
zo	20.0279	16.6194	20.0533	16.6240	16.7600
rma	105.044	105.044	104.935	104.935	103.320
a	13.00	12.00	13.00	12.00	12.00
b	14.00	19.00	14.00	19.00	19.00
c	42.00	42.00	42.00	42.00	42.00
zh	57.652	57.652	57.652	57.652	57.652

Tab. 1 Geometry parameters of different half cells (ee: end half cell end resonator, ei: intermediate half cell end resonator, se: end half cell inner resonator, si: intermediate half cell inner resonator, in: inner cell any resonator); all quantities given in mm; data provided from Sekutowicz [7] with exception of rma(ee), ro(ee) and zo(ee) which have been modified to improve the calculated field flatness.

The positions of the r-mesh lines were chosen in such a manner that all the specific points of the shape (rw, ru, ro, ...) were hit exactly. The number of lines between them was fixed in a way to achieve similar mesh sizes - at least locally. There was no automatism used to do this for two reasons:

- The distances between the specific points vary in a broad range.
- The slope of the shape is partly (near iris and equator) near to zero and the z-lines are spread very wide; in the linear part the slope is very high and z-lines are close together.

As a consequence of both reasons, the ratio of mesh sizes becomes quite high globaly (in the order of 50) and one has to take care to keep it locally significantly below 10. One important measure to do so

is a selection of r-mesh positions in the elliptic and circular part, calculated from steps of equal angles (seen from the center of the resp. shape). This results in small ratios of mesh sizes from step to step, as well in z- as in r-direction (comp. fig. 3).

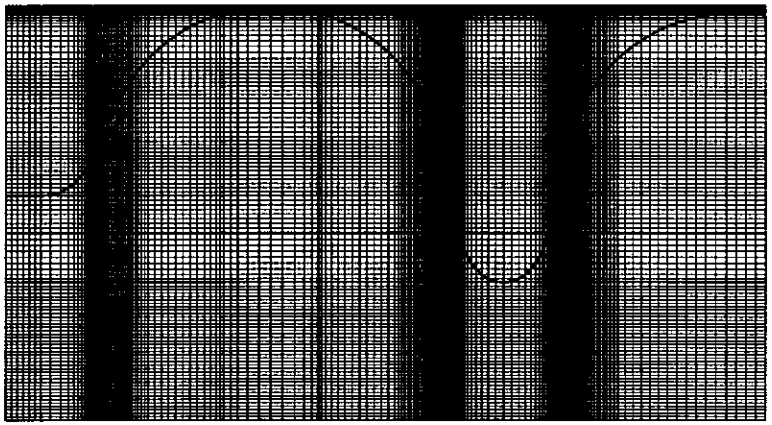

Fig. 3: Part of grid and shape near the left end of the structure. The second cell has a smaller equator radius which makes additional r-mesh lines necessary. The density of z-mesh lines has its highest values in the areas with highest cavity boundary slopes and vice versa.

Using a grid of 241000 mesh points constructed in the descibed manner the eigenfrequencies and eigenmodes of the 2x7-chain have been calculated in two runs for both the electric and the magnetic boundary condition at the right end, corresponding to the symmetry plane of the complete 4x7-structure. In either run the first 42 monopol modes have been calculated; the first 14 modes of both runs together give the 28-mode fundamental passband. Its so called π-0-mode is the accelerating one, which is found as mode no. 13 of the run with electrical boundary conditions.

Since the original geometry data showed poor field flatness in the outer cavities the equator radius of the outermost end cells has been changed. In Fig. 4 a-d the field profiles of the accelerating mode are shown for equator radii of 104.935 mm, 104.994 mm, 105.044 mm and 105.094 mm. The run with the radius of 105.044 mm was used, even if there might still be some slight field flatness improvement possible.

The eigenfrequencies, stored field energies and on-axis field profiles were extracted with the MAFIA-post-processor. All further calculations have been done with a special code (M. Dohlus) or *Mathematica*™. For the reason of comparison the whole procedure has been repeated with a standard 9-cell-structure.

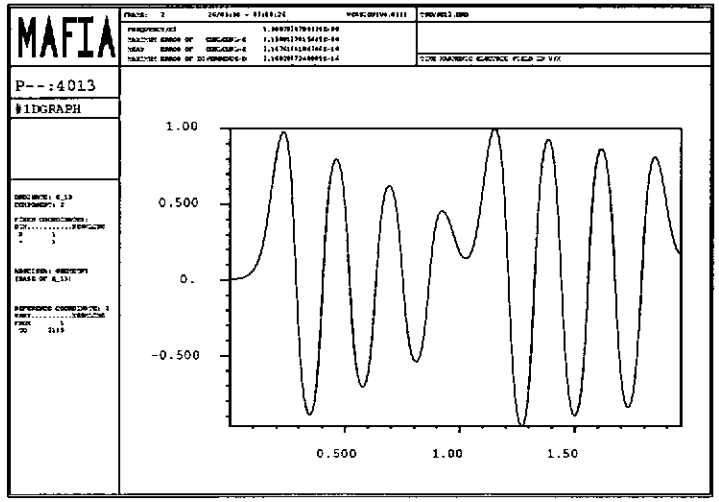

Fig. 4 a: On-axis profile of E_Z-field of the accelerating mode for 104.935 mm equator radius of the left end cell.

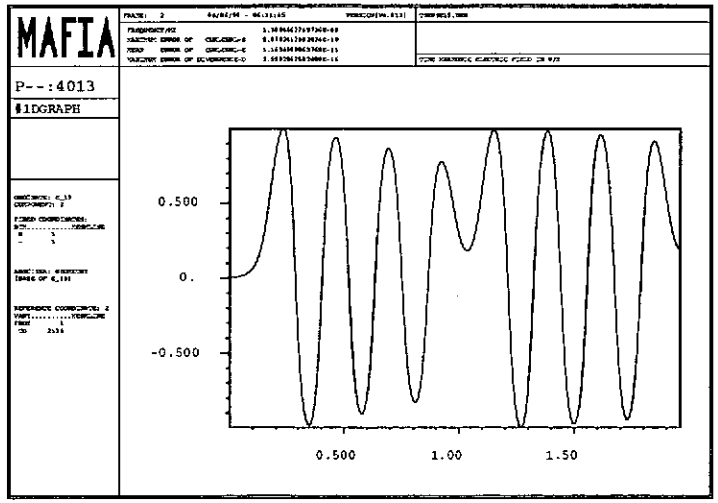

Fig. 4 b: On-axis profile of E_Z-field of the accelerating mode for 104.994 mm equator radius of the left end cell.

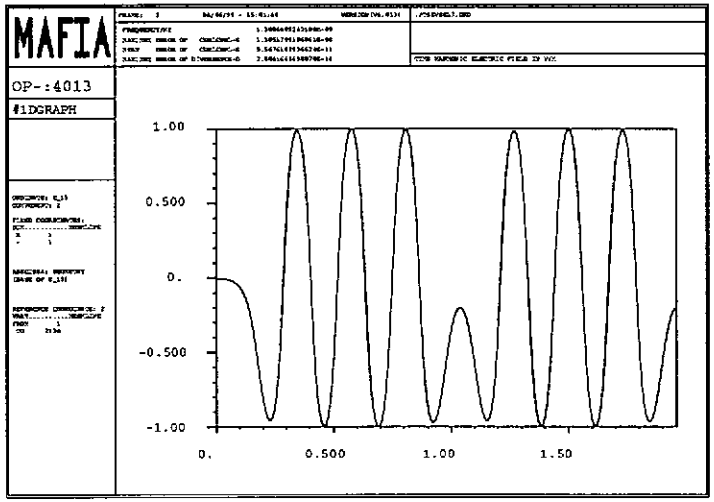

Fig. 4 c: On-axis profile of E_z-field of the accelerating mode for 105.044 mm equator radius of the left end cell; this run was used for further calculations.

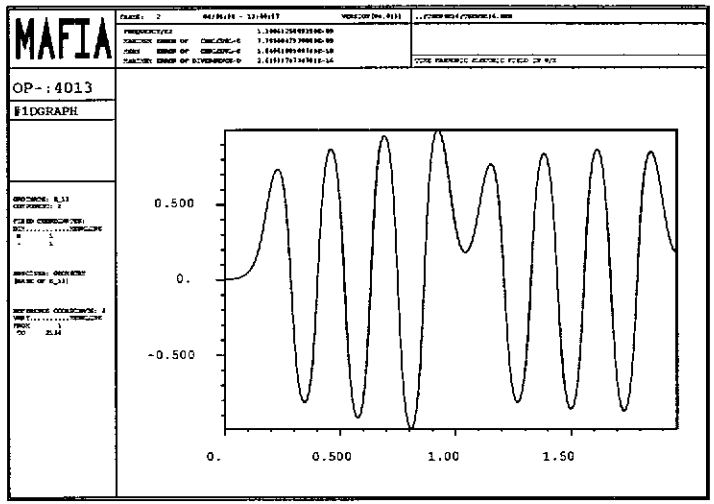

Fig. 4 d: On-axis profile of E_z-field of the accelerating mode for 105.094 mm equator radius of the left end cell.

4. Time Dependent Field Amplitudes in TESLA-9-Cell- and 4x7-Cell-Structure

In order to calculate the temporal behaviour one has to perform the following steps:

- Determine the coupling K_ν from the transmitter to each mode according to (11) and set up the vector $\vec{K}$ from (32) using the field profiles, frequencies and stored energy data from the MAFIA-calculation.
- Build the system matrix $\underline{M}$ given in (19) from K_ν and the MAFIA eigenfrequencies. Start with a typical transmitter impedance R and calculate the eigenvalues of the system matrix. Compare the Q-value of the accelerating mode found from (43) with the goal for Q, given from the demanded filling time. Fit R accordingly, applying the (almost) linear dependency $Q \sim R$. Calculate and keep all the eigenvalues and eigenvectors of this final system matrix. Set up the column matrix $\underline{V}$ of the eigenvectors following (25).
- For each pair of indices (j, ν) calculate the integral expression in (38), using the field profiles and the eigenvalues of the system matrix. Store these values.
- Use (41) to calculate the eigenmode amplitudes $a_\nu(t)$ if no beam excited the cavities prior to the calculation time t. Otherwise apply (40), which needs the summation over all previous bunches, performed in (39), and the transmitter excitation, expressed in (33). To calculate the beam excitation the time of entering the cavity t_b has to be known for each bunch. The charges of the bunches are assumed to be equal to q for all bunches, which is then used as a common factor.
- Repeat the last step for every point of time t the field distribution is asked for. The total field is found from the series expansion (3) using the coefficients $a_\nu(t)$ with the MAFIA field profiles and energies.

In the TESLA scheme 1130 bunches of 5.7267 nC charge are foreseen following each other in a distance of 919 rf periods. The injection of the first bunch happens at rf period 760336 (584.6 μs) at half the unloaded steady state voltage. From this an external Q = 3446120 follows. This data allows to calculate the transmitter resistance, which of course is only valid for a certain coupling, defined by length and position of the current path. For the calculations in Fig. 5 a (slightly to low) Q = 3433810 was found from the $\underline{M}$-eigenvalue λ_j using (43). This results in a voltage decrease (cf. Tab. 2) during the bunch train and is cited here to illustrate the dependencies. The voltage was calibrated to be 25 MV/m inside the resonators at first injection, equal to 80.6756 MV in total for the 4x7-structure.

Ez/(MV/m)	cell 1	cell 7	cell 28
bunch 1	47.352	48.009	47.426
bunch 1130	47.089	47.831	47.044
decrease	-0.55%	-0.37%	-0.80%

Table 2: Decrease of accelerating voltage in the 4x7-structure in the case of a slight mismatch of the transmitter resistance, i.e. coupling (ext. Q = 3433810 instead Q = 3446120).

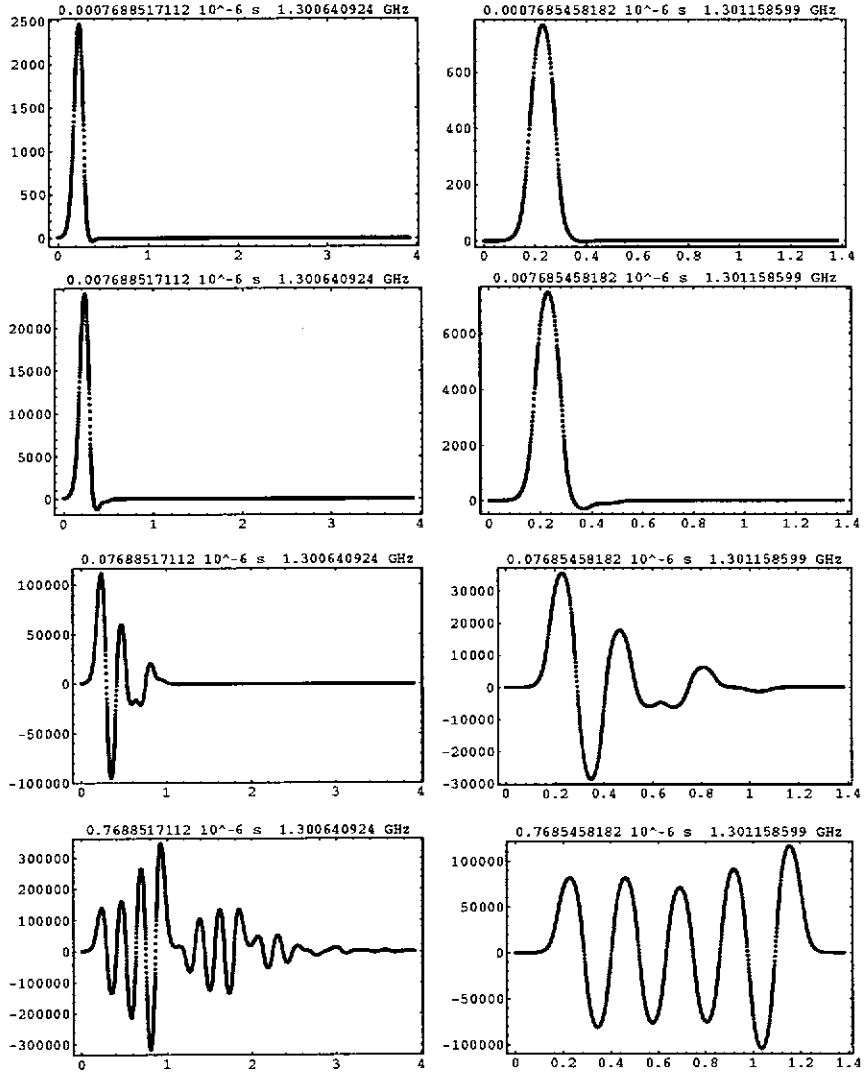

Fig. 5 a (left column), b (right column): On-axis Ez field profiles of the 4x7-cell-superstructure (left) and the 9-cell-structure (all pictures: Ez/(V/m) vs. length/m) after 1, 10, 100, 1000 rf-periods. During these early phase field profiles of both structure types correspond very well (picture continued on following page).

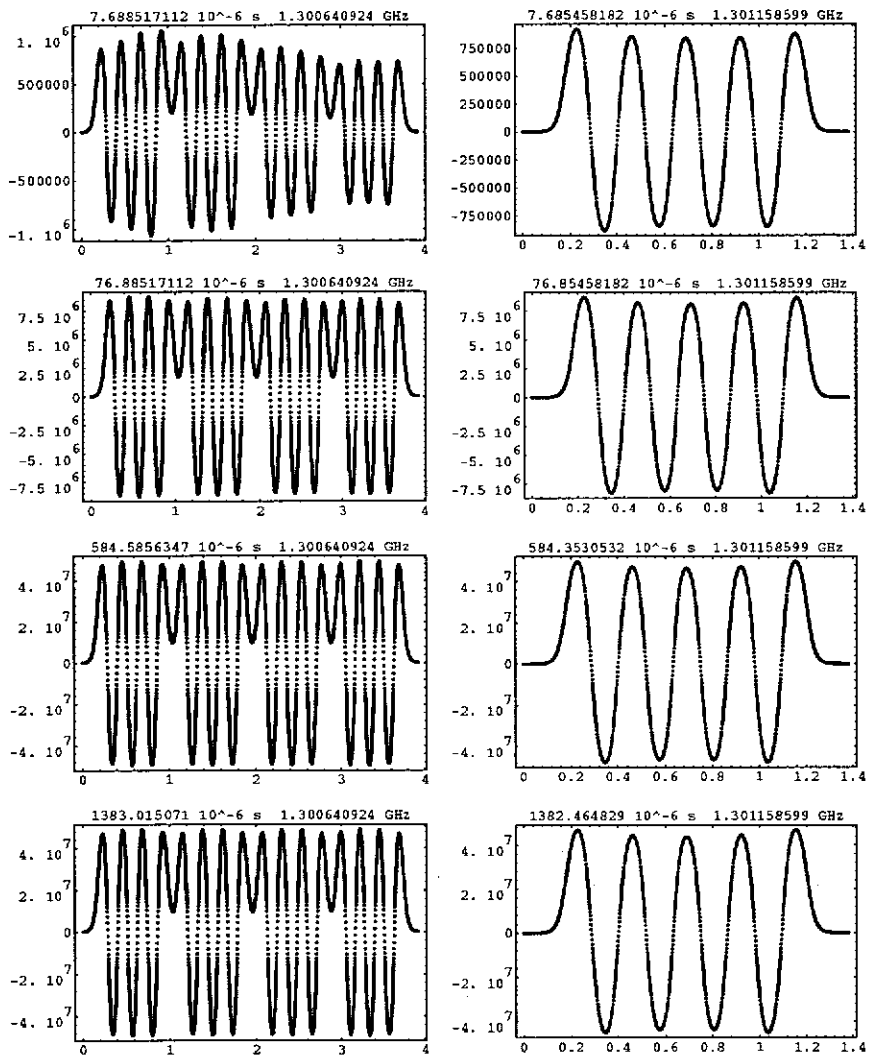

Fig. 5 a (left column), b (right column) (picture continued from previous page): On-axis Ez field profiles of the 4x7-cell-superstructure (left) and the 9-cell-structure (all pictures: Ez/(V/m) vs. length/m) after 10000, 100000, 760336 (first bunch), 2037236 (last bunch of 1130) rf-periods. The field distribution of the long structure stabilizes later than the one of the 9-cell-structure. In either case the distribution is stable and the amplitude has its target value when the beam enters the cavities. Both remain unchanged (as far as it can be seen for this picture scaling) during the time of the bunch train passin g the structure.

Fig. 5 illustrates one main result of the work, showing series of snap shots of the on-axis z-component of the electrical field along both a superstructure and a 9-cell-structure. As one would expect the build-up of a flat field distribution takes longer in the superstructure, but for both structure types the field geometry stabilizes fast enough and reaches the demanded amplitude, too. Furthermore, during the passage of the bunch train the fields are kept stable (in the range visible in Fig. 5). This confirms a sufficient energy transport even through the long cavity chain.

In Fig. 6 the on-axis field strength of the last cell (no. 28) is shown for various moments in time. The field rises up in the expected manner. The complicated time behaviour in the very beginning is not visible in the scale used here. The beam is injected at 50% of the steady state voltage. From then on the amplitude remains stable even in the chosen cell having the biggest distance to the input coupler.

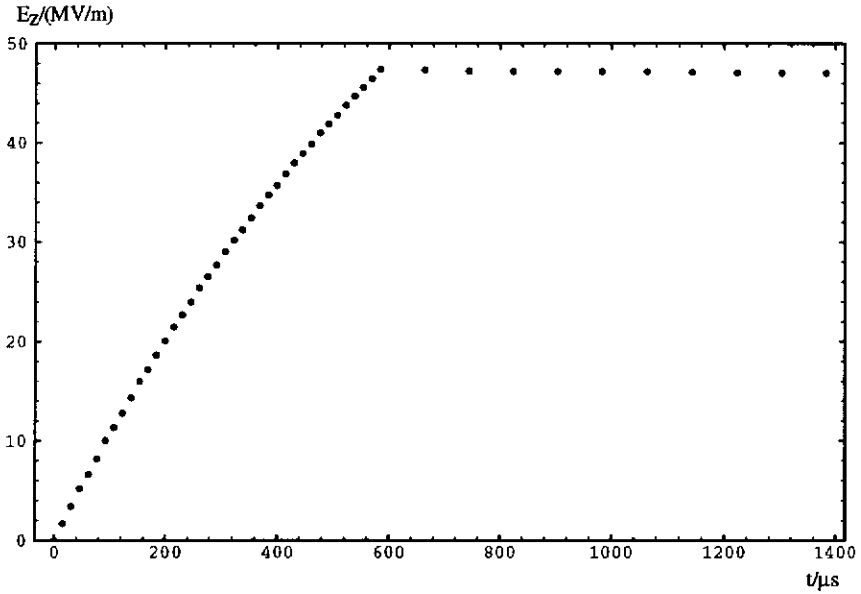

Fig. 6 Z-component of the accelerating on-axis Ez-field in the center of the last cell of the 4x7-structure vs. time. Even in this cell with the largest distance to the input coupler, the field amplitude remains stable (beside the weak decrease mentioned in Tab. 2, caused by a slightly mismatched Q) during the bunch train traversal (584 μs < t < 1386 μs). The beam is injected at half the steady-state voltage.

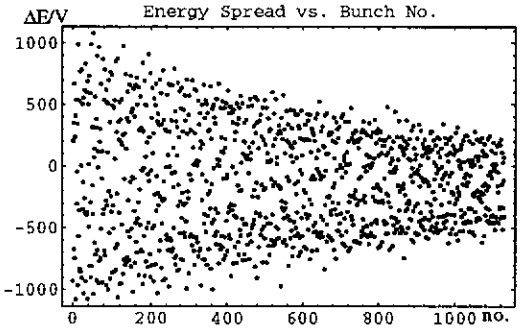

Fig. 7 Deviation of integrated accelerating field of the superstructure from average value of 80.6756 MV vs. bunch number. Data were calculated without simplification and therefore incorporating the influence of the actual bunch in the cavity.

Fig. 7 contains the total energy gain of each bunch that passed the superstructure. The remaining jitter is smaller than 1100 V compared to the average value of 80.6756 MV.

5. Conclusions

The modal expansion is a useful method to calculate non-stationary fields for time intervalls much longer than those which may be calculated directly in time domain.

A special grid, generated (almost) automatically approximates the shape of TESLA-type resonators without staircases with a reasonable number of mesh points.

The 4x7-superstructure has a slower filling and refilling than the 9-cell resonator (as one would expect) but fast enough for proper operation.

References

[1] MAFIA V. 4.015, CST, D-64289 Darmstadt

[2] M. Dohlus, R. Schuhmann, T. Weiland: "Calculation of Frequency Domain Parameters Using 3D Eigensolutions", International Journal of Numerical Modelling: Electronic Networks, Devices and Fields (invited, to be published)

[3] M. Ferrario, A. Mosnier, L. Serafini, F. Tazzioli, J.-M. Tessier, "Multi-Bunch Energy Spread Induced by Beam Loading in a Standing Wave Structure", Part.Acc. 52 (1996), pp. 1-30

[4] H.-W. Glock, P. Hülsmann, M. Kurz, H. Klein: "Rise Time of Amplitudes of Time Harmonic Fields in Multicell Cavities", Proc. 1993 Particle Accelerator Conference, May 1993, Washington D.C., pp. 623-625

[5] J. Sekutowicz, M. Ferrario, C. Tang: Superconducting Superstructure; LC97, Sept./Oct. 97, Zvenigorod, Russia

[6] J. Sekutowicz, M. Ferrario, C. Tang: "Superconducting Superstructure for the TESLA Collider", TESLA-Report 98-08, DESY, April 1998

[7] J. Sekutowicz, priv. comm.